Supporting Information

Reactive processing of formaldehyde and acetaldehyde in aqueous aerosol mimics: Surface tension depression and secondary organic products

*Zhi Li, Allison N. Schwier, Neha Sareen, V. Faye McNeill**

Department of Chemical Engineering, Columbia University, New York, NY, 10027, USA

* To whom correspondence should be addressed. Email: vfm2103@columbia.edu

Table S1. Calculated errors between the Henning model predictions (using eq. (3)) and experimentally measured surface tension values.

Total Organic Concentration	Species	MG*	Acet*	Form*	Model Prediction	Measured Data	Error
(mol/L)		(mol C/kg H_2O)			(dyn cm^{-1})		(%)
0.05	MG Acet:Form=1:3	0.030	0.020	0.030	73.848	67.438	8.680
		0.060	0.015	0.022	69.730	64.438	7.589
		0.090	0.010	0.015	66.454	61.822	6.970
		0.120	0.005	0.007	63.712	59.159	7.146
	MG Acet:Form=1:1	0.113	0.013	0.006	64.832	60.105	7.292
		0.075	0.025	0.012	68.868	63.105	8.368
		0.038	0.038	0.019	73.673	68.249	7.362
	MG/Acet	0.038	0.075	N/A	75.081	66.407	11.553
		0.075	0.051	N/A	70.361	62.575	11.066
		0.113	0.025	N/A	65.746	60.465	8.032
0.5	MG/Acet	1.153	0.259	N/A	55.433	47.388	14.512
		0.770	0.518	N/A	62.788	50.389	19.747
		0.385	0.778	N/A	70.895	54.454	23.190
	MG/Form	1.148	N/A	0.126	51.809	48.046	7.263
		0.763	N/A	0.252	55.868	50.638	9.361
		0.381	N/A	0.377	62.142	56.334	9.346

*MG: Methylglyoxal; Acet: Acetaldehyde; Form: Formaldehyde

Density functional theory calculations of paraformaldehyde ionization by I^-

Density functional theory calculations were used to evaluate the thermodynamic favorability of the following chemical ionization reaction for paraformaldehyde (n = 9):

$$I^- + R{-}OH \rightarrow R\text{-}O^- + HI \qquad (S1)$$

Geometry optimizations and energy calculations were performed using Jaguar 7.7 (Schrödinger, Inc.). The B3LYP functional was used with the ERMLER2 basis set, which allows the treatment of iodine via the use of effective core potentials (Lajohn et al., 1987). The results of the calculation are shown in Table S2. We found that reaction S1 is thermodynamically favorable, with ΔG = -4.99 kJ mol^{-1}. We believe that the ionized species is stabilized by interactions between the ionized $-O^-$ and the other terminal hydroxyl group(s) on the molecule (see the optimized geometry in Figure S1).

Table S2. Calculated total Gibbs free energy.

Species	Gtot (Hartrees)
I-	-111.5214881
Paraformaldehyde (n= 9)	-1106.4844260
Ionized paraformaldehyde (n = 9)	-1105.9625590
HI	-112.0452540

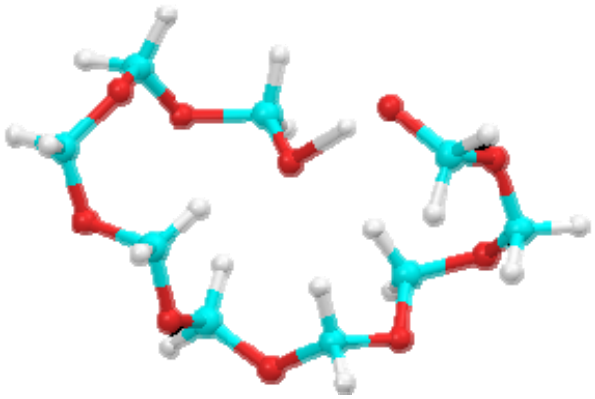

Figure S1. Optimized structure of ionized paraformaldehyde (n = 9). White = H, red = O, cyan = C.

Table S3. Proposed peak assignments for Aerosol-CIMS mass spectra with H_3O^+ of atomized solutions of 1 M formaldehyde in 3.1 M AS.

m/z (amu) ± 1.0 amu	Ion Formula	Molecular Formula	Possible Structures	Mechanism
77.2	$C_2H_5O_3^+$	$C_2H_4O_3$	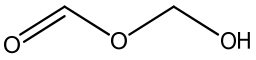	hemiacetal
94.9	$C_2H_5O_3^+ \cdot H_2O$	$C_2H_4O_3$	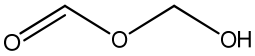	hemiacetal
	$C_2H_7O_4^+$	$C_2H_6O_4$	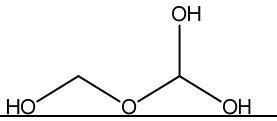	
107	$C_3H_7O_4^+$	$C_3H_6O_4$	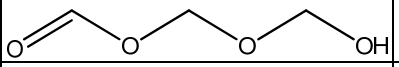	hemiacetal
113.2	$C_2H_5O_3^+ \cdot 2H_2O$	$C_2H_4O_3$	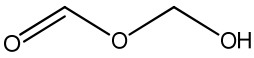	hemiacetal
	$C_2H_7O_4^+ \cdot H_2O$	$C_2H_6O_4$	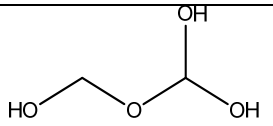	
124.9	$C_3H_7O_4^+ \cdot H_2O$ $C_3H_9O_5^+$	$C_3H_6O_4$ $C_3H_8O_5$	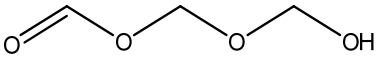	hemiacetal
137	$C_4H_9O_5^+$	$C_4H_8O_5$	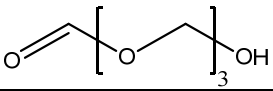	hemiacetal
143.5	$C_3H_7O_4^+ \cdot 2H_2O$ $C_3H_9O_5^+ \cdot H_2O$	$C_3H_6O_4$ $C_3H_8O_5$	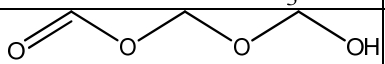	hemiacetal

Table S4. Proposed peak assignments for Aerosol-CIMS mass spectra with H_3O^+ of atomized solutions of 0.5 M formaldehyde/MG (1:1) in 3.1 M AS.

m/z (amu) ± 1.0 amu	Ion Formula	Molecular Formula	Possible Structures	Mechanism
84.3	$CH_3O_2^+ \cdot 2H_2O$	CH_2O_2	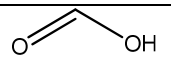	Formic Acid
	$CH_5O_2^+ \cdot 2H_2O$	CH_4O_2	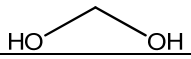	Hydrated F
96.1	$C_2H_5O_3^+ \cdot H_2O$	$C_2H_4O_3$	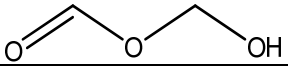	hemiacetal
125.1	$C_3H_7O_4^+ \cdot H_2O$	$C_3H_6O_4$	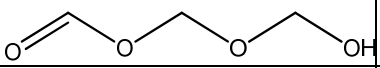	hemiacetal
154.9	$C_4H_9O_5^+ \cdot H_2O$	$C_4H_8O_5$	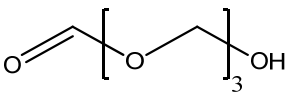	n=4 hemiacetal

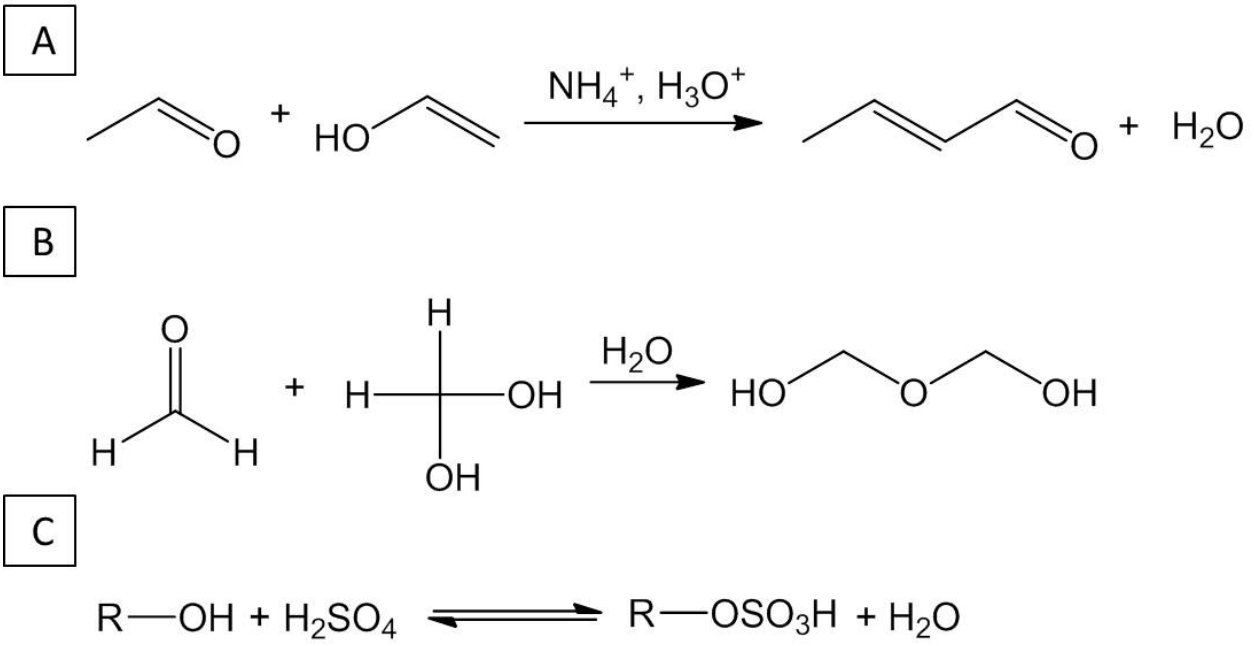

Figure S2. Main reaction pathways of A) aldol condensation catalyzed by NH_4^+ or H_3O^+ ; B) hemiacetal formation; C) alcohol sulfate ester formation.

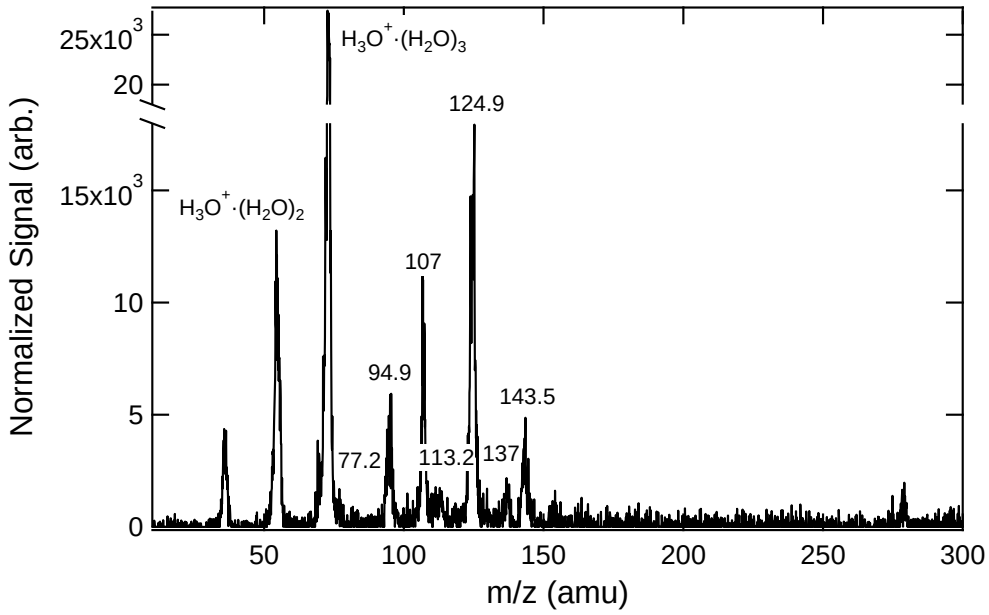

Figure S3. Aerosol CIMS spectra of atomized solutions of 1 M formaldehyde in 3.1 M AS. See the text for details of sample preparation and analysis. Positive-ion mass spectrum obtained using $H_3O^+\cdot(H_2O)_n$ as the reagent ion.

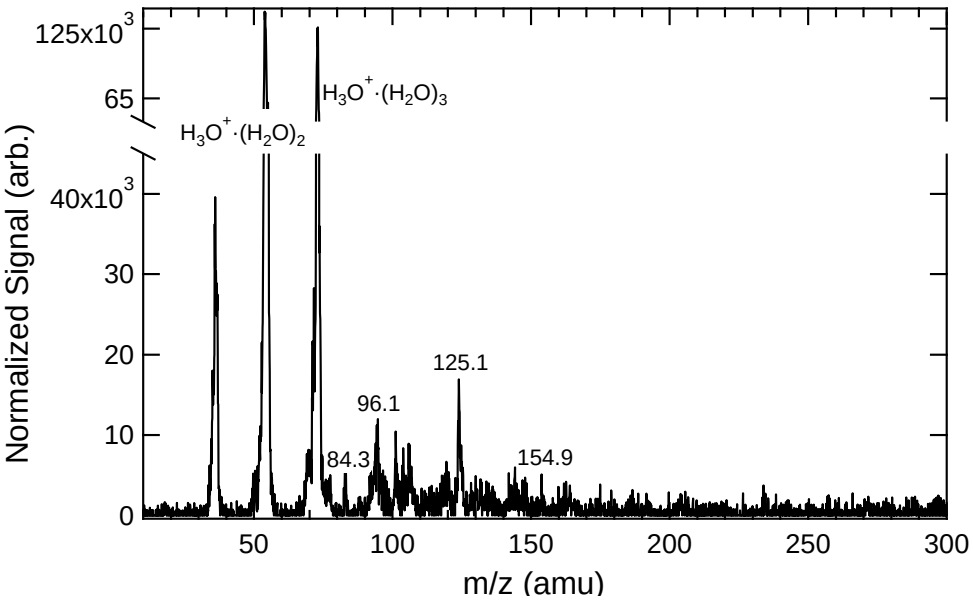

Figure S4. Aerosol CIMS spectra of atomized solutions of 0.5 M formaldehyde/MG (1:1) in 3.1 M AS. See the text for details of sample preparation and analysis. Positive-ion mass spectrum with $H_3O^+ \cdot (H_2O)_n$ as the reagent ion.

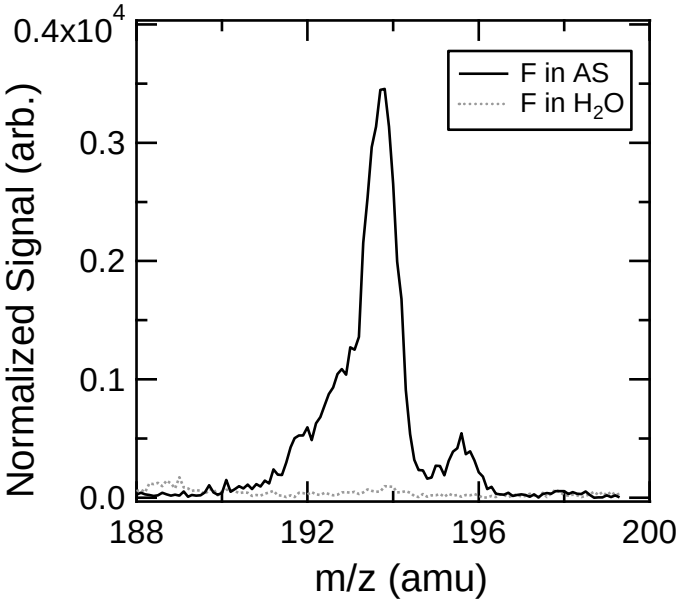

Figure S5. Aerosol CIMS spectra showing a closeup of the possible organosulfate peak (m/z 193.8) identified in the 0.2 M formaldehyde in 3.1 M AS solution in negative-ion mode. The satellite peak (m/z 195.6) is also visible.

Predictions of paraformaldehyde sulfate ester production

We attribute the signal at 193.8 amu in the formaldehyde/AS spectrum to an organosulfate derived from the formaldehyde hemiacetal dimer ($C_2H_6O_6S$). After 24 h of reaction, the mass spectrum shows signal of 3500 counts/s at this mass. Assuming an upper bound sensitivity of 100 counts s^{-1} ppt^{-1} for this species (Sareen et al., 2010), and based on the volume weighted geometric mean diameter of 414(±14) nm and the average particle concentration of ~4×10^4 cm^{-3}, we estimate a lower limit for the in-particle concentration of this species to be ~10^{-3} M. Taking into account the concentrating effect of aerosol dehydration after atomization and dilution of the aerosol stream with dry N_2, we infer a $C_2H_6O_6S$ concentration of $\geq2\times10^{-4}$ M in the bulk solution after 24 h of reaction.

According to Deno and Newman the formation of alcohol ester sulfates occurs via the reaction with H_2SO_4, not SO_4^{-2} or HSO_4^- (Deno and Newman, 1950). We assume here that the same is true for the formation of $C_2H_6O_6S$ from $C_2H_6O_3$. Minerath and coworkers reported that sulfate esterification of ethylene glycol, a close structural analog of $C_2H_6O_3$, occurred in 75 wt% H_2SO_4 according to:

$$C_2H_6O_2 + H_2SO_4 \leftrightarrow C_2H_6O_5S + H_2O \quad \text{(S2)}$$

with a forward pseudo-first-order rate constant of 7.30×10^{-4} s^{-1} and reverse pseudo-first-order rate constant of 3.00×10^{-4} s^{-1} (Minerath et al., 2008). This translates to a forward second-order rate constant of 6.29×10^{-5} $M^{-1}s^{-1}$ and reverse second-order rate constant of 1.43×10^{-5} $M^{-1}s^{-1}$.

The following reaction was modeled using POLYMATH 6.10:

$$2\ HCHO\ (+H_2O) \rightarrow C_2H_6O_3 \quad \text{(S3)}$$

$$C_2H_6O_3 + H_2SO_4 \leftrightarrow C_2H_6O_6S + H_2O \quad \text{(S4)}$$

With $k_{S4} = 6.29\times10^{-5}$ $M^{-1}s^{-1}$ and $k_{-S4} = 1.43\times10^{-5}$ $M^{-1}s^{-1}$. Formaldehyde dimerization is assumed to be fast, with a rate constant similar to glyoxal dimerization (pseudo first-order rate constant = 5×10^{-4} s^{-1} (Fratzke and Reilly, 1986)). We found that the model was insensitive to this parameter, because reaction (S4) was rate-limiting. Based on this model we predict a maximum $C_2H_6O_6S$ concentration of ~7×10^{-8} M after 24 h of reaction. This calculation provides an upper bound estimate of $C_2H_6O_6S$ concentration since other sinks for formaldehyde monomer and $C_2H_6O_3$

exist in the system which are not represented by this simple model. Nevertheless, this model underpredicts the observed $C_2H_6O_6S$ concentration by a factor of $\geq$3000. This disagreement between model and experiment suggests that either a) the kinetics of sulfate esterification for paraformaldehyde are significantly faster than for alcohols b) SO_4^{-2} or HSO_4^- is the active reactant, contrary to the conclusions of Deno and Newman, or c) sulfate esterification is enhanced by the solution dehydration that accompanies the atomization and volatilization steps in our detection technique.

REFERENCES

Deno, N. C. and Newman, M. S.: Mechanism of Sulfation of Alcohols, *J. Am. Chem. Soc.*, *72* (9), 3852-3856, 1950.

Fratzke, A. R. and Reilly, P. J.: Thermodynamic and Kinetic Analysis of the Dimerization of Aqueous Glyoxal, *Int. J. Chem. Kinetics*, *18,* 775-789, 1986.

Lajohn, L. A., Christiansen, P. A., Ross, R. B., Atashroo, T., and Ermler, W. C.: Abinitio Relativistic Effective Potentials with Spin Orbit Operators .3. Rb Through Xe, *J. Chem. Phys.*, *87* (5), 2812-2824, 1987.

Minerath, E. C., Casale, M. T., and Elrod, M. J.: Kinetics feasibility study of alcohol sulfate esterification reactions in tropospheric aerosols, *Environ. Sci. Technol.*, *42* (12), 4410-4415, 2008.

Sareen, N., Schwier, A. N., Shapiro, E. L., Mitroo, D. M., and McNeill, V. F.: Secondary organic material formed by methylglyoxal in aqueous aerosol mimics, *Atmos. Chem. Phys.*, *10*, 997-1016, 2010.